

Deep subspace encoders for continuous-time state-space identification

Gerben Izaak Beintema¹, Maarten Schoukens¹, and Roland Tóth^{1,2}

¹ Department of Electrical Engineering, Eindhoven University of Technology, Eindhoven, The Netherlands `\{g.i.beintema,m.schoukens,r.toth\}@tue.nl`

² Systems and Control Laboratory, Institute for Computer Science and Control, Budapest, Hungary.

Abstract. Continuous-time (CT) models have shown an improved sample efficiency during learning and enable ODE analysis methods for enhanced interpretability compared to discrete-time (DT) models. Even with numerous recent developments, the multifaceted CT state-space model identification problem remains to be solved in full, considering common experimental aspects such as the presence of external inputs, measurement noise, and latent states. This paper presents a novel estimation method that includes these aspects and that is able to obtain state-of-the-art results on multiple benchmarks where a small fully connected neural network describes the CT dynamics. The novel estimation method called the subspace encoder approach ascertains these results by altering the well-known simulation loss to include short subsections instead, by using an encoder function and a state-derivative normalization term to obtain a computationally feasible and stable optimization problem. This encoder function estimates the initial states of each considered subsection. We prove that the existence of the encoder function has the necessary condition of a Lipschitz continuous state-derivative utilizing established properties of ODEs.

Keywords: Continuous-time identification · State-space identification.

1 Introduction

Dynamical systems described by nonlinear state-space models with a state vector $x(t) \in \mathbb{R}^{n_x}$ are a major tool of many modern sciences and engineering disciplines to understand potentially complex dynamical systems. One can distinguish between Discrete-Time (DT) $x_{n+1} = f(x_n)$ and Continuous-Time (CT) $\frac{dx(t)}{dt} = f(x(t))$ state-space models. In general, obtaining DT dynamical models from data is easier than CT models since modern computers are finite-state machines. However, the additional implementation complexity and computational costs associated with identifying CT models can be justified in many cases. First and foremost, from the natural sciences, we know that many systems are compactly described by CT dynamics which makes the continuity prior of CT models a well-motivated regularization. It has been observed that this regularization can be beneficial for sample efficiency [11] which is a common observation

when “including physics” in learning approaches [18]. Furthermore, the analysis of ODE equations is a well-regarded field of study with many powerful results and methods which could further improve model interpretability [12], such as applied in [3]. Another inherent advantage is that these models are able to incorporate irregular sampled or missing data [27]. Finally, in the control community, CT models are generally regarded as desirable for control synthesis tasks [14]. Hence, we argue that developing robust and general CT models and estimation methods would be greatly beneficial.

In practical CT identification problems like [30] it is common to encounter aspects such as: external inputs ($u(t)$), noisy measurements, latent states, unknown measurement function/distribution (e.g. $y(t) = h(x(t))$), the need for accurate long-term predictions and a need for a sufficiently low computational cost. Many of these aspects have been studied independently in quite some detail, for instance, [6,27] explicitly addressed the presence of noise on the measurement data, [21,9] provided methods for modeling dynamics with latent states, [33] considers the presence of known external inputs, [34] provides a computationally tractable method for accurate long-term sequence modeling. However, formulating models and estimation methods for the combination of multiple or all aspects is in comparison underdeveloped with only a few attempts [13].

In contrast to previous work, we present the CT encoder method which is a general, robust and well-performing estimation method for CT state-space model identification. That is, the formulation addresses noise assumptions, external inputs, latent states, an unknown output function, and provides state-of-the-art results on multiple benchmarks. Moreover, we attain additional novelty as these results are obtained without needing to impose a specific structure (e.g. [16,10]) on the state-space obtaining a widely applicable method.

Our main contributions are the following;

- We formally derive the problem of CT model estimation with latent states, external inputs, and measurement noise.
- We reduce the computational loads by proposing the subspace encoder identification algorithm that employs short subsections, an encoder function that estimates the initial latent states of these subsections, and a state-derivative normalization term.
- Using conventional ODE analysis, we show that the encoder function approximates the well-known reconstructability map which is ordinarily impractical to compute analytically when considering nonlinear dynamics described by neural networks. We also show that a necessary condition of the existence of the encoder function is that the state-derivative function (f) is Lipschitz continuous.
- We demonstrate that the proposed estimation method obtains state-of-the-art results on multiple benchmarks.

2 Related work

One of the most influential papers in this research direction is the neural ODE contribution [9] which showed that residual networks can be viewed as an Euler discretization of a continuous in-depth neural network. Moreover, they also show that one is able to employ numerical integrators to integrate through depth in a computationally efficient manner. They also proposed that this depth can be interpreted as the time direction to be able to model dynamical systems. However, this approach does not scale well to long sequences, nor does it consider external inputs or noise, and the resulting optimization problem is often unstable. The ideas in the neural ODE contribution have been extended to/used in, for instance, normalizing flows to efficiently model arbitrary probability distributions [23,15], and enhanced the understanding and interpretability of neural networks of various kinds [12].

An adjacent research direction is the method/models which consider CT dynamics and directly use the state derivatives and often the noiseless states to formulate structured and interpretable models such as Hamiltonian Neural Networks (HNN) [16], Lagrangian Neural Networks (LNN) [10] and Sparse Identification of Nonlinear Dynamics (SINDy) [7]. In contrast, the proposed method is formulated for an unstructured state-space and will not require the system state or the state derivatives to be known.

Our method is most directly related to [2] which concerns the estimation of CT models with latent variables. Curiously, they also employ an encoder function (with different input parameters) but they do not elaborate on its introduction. However, they only consider a fixed output function and solve their optimization problem as an optimal control problem whereas our formulation alters the simulation loss function to obtain the computationally desirable form. Furthermore, [13], to which we compare in this work, considers a CT model with latent variables, time series subsections, and an additional loss term for the integration error. However, they include the initial states of these subsections as free optimization parameters, and, hence, this will increase the model complexity with the number of subsections. In contrast, our proposed method uses an encoder to estimate the initial states which has a fixed model complexity and we only employ a single loss function.

3 Background

Consider a system represented by the following continuous-time state-space description:

$$\begin{aligned}\dot{x}_s(t) &= f(x_s(t), u(t)), \\ \bar{y}(t) &= h(x_s(t), u(t)),\end{aligned}\tag{1}$$

where $x_s(t) \in \mathbb{R}^{n_{xs}}$ is the system state variable, $u(t) \in \mathbb{R}^{n_u}$ the input, $\bar{y}(t) \in \mathbb{R}^{n_y}$ the noiseless output, f represents the system dynamics and h the output function. For simplicity of notation we assume that h is independent of $u(t)$.

Measurements of the system are obtained by sampling the system output at a certain sample time Δt (assumed fixed for simplicity)

$$y_n = y(n\Delta t) = \bar{y}(n\Delta t) + w_n,$$

The measurements are corrupted by unknown zero-mean noise $w_n \in \mathbb{R}^{n_y}$ with finite variance Σ_w . This noise is assumed to be white on the timescale of Δt (i.e. $\mathbb{E}[w_n w_{n+k}] = 0, \forall k \neq 0, k \in \mathbb{Z}, n \in \mathbb{Z}$).

With these definitions the CT model estimation problem can be expressed as; for a given dataset of measurements:

$$D_N = \{(u(0), y(0)), (u(\Delta t), y(\Delta t)), \dots, (u((N-1)\Delta t), y((N-1)\Delta t))\},$$

with potentially unknown w_n , $x_s(t)$, $\dot{x}_s(t)$ and initial state $x_s(0)$, the task is to solve the following optimization problem (a.k.a. simulation loss minimization):

$$\begin{aligned} \min_{\theta, x(0)} \quad & \frac{1}{N} \sum_{k=0}^{N-1} \|y(k\Delta t) - \hat{y}(k\Delta t)\|_2^2, \\ \text{s.t.} \quad & \hat{y}(t) = h_\theta(x(t)), \\ & \dot{x}(t) = f_\theta(x(t), u(t)), \end{aligned} \tag{2}$$

where $x(t) \in \mathbb{R}^{n_x}$ is the model state, h_θ and f_θ are Lipschitz continuous functions parameterized by θ . To obtain the simulation output $\hat{y}(k\Delta t)$ one can integrate $\frac{dx(t)}{dt} = f_\theta(x(t), u(t))$ starting from the given initial state $x(0)$. This integration can be performed with any ODE solver which allows for back-propagation such as Euler ($x(t + \Delta t) = x(t) + \Delta t f_\theta(x(t), u(t))$), RK4 or numerous adaptive step methods [9,25]. To make this a well-posed optimization problem, additional information or an assumption on the inter-sample behaviour of $u(t)$ is required, since, for example $u(\Delta t/2)$ is not present in D_N . This behaviour is often chosen to be Zero-Order Hold (ZOH) (i.e. $u(k\Delta t + a) = u(k\Delta t), \forall a \in [0, \Delta t), k \in \mathbb{Z}$).

Solving the optimization problem (2) with a gradient-descent based method is problematic in many situations. A major problem is that computing the value of the loss function requires a forward pass on the whole length of the dataset [2]. Hence, the computational complexity will grow linearly with the length of the dataset. Furthermore, a common occurrence is that the values of $x(t)$ or its gradient grows exponentially which causes the loss function or its gradients to be non-smooth. This often causes gradient-based optimization algorithms to become unreliable since the optimization process might be unstable or converge to a local minima [25].

4 Proposed method

We propose to consider multiple potentially overlapping short subsections of length $T\Delta t$ to form a truncated simulation loss instead of simulating over the

entire length of the dataset. We express this in the following optimization problem (note that we express the optimization problem with discrete-time notation ($u_k := u(k\Delta t)$) for brevity):

$$\begin{aligned}
 \min_{\theta} \quad & \sum_{n=\max(n_a, n_b)}^{N-T} \sum_{k=0}^{T-1} \|y_{n+k} - \hat{y}_{n+k|n}\|_2^2, \\
 \text{s.t.} \quad & \hat{y}_{n+k|n} = h_{\theta}(x_{n+k|n}), \\
 & x_{n+k+1|n} = \text{ODEsolve}\left[\frac{1}{\tau} f_{\theta}, x_{n+k|n}, u_{n+k}, \Delta t\right], \\
 & x_{n|n} = \psi_{\theta}(u_{n-1}, \dots, u_{n-n_b}, y_{n-1}, \dots, y_{n-n_a}).
 \end{aligned} \tag{3}$$

Here, the pipe (|) notation indicates the current index and the starting index as (Current index | Start index) to differentiate between different subsections. Furthermore, ODEsolve indicates a numerical scheme which integrates $1/\tau f_{\theta}(x, u)$ from the initial state $x_{n+k|n}$ for a length of Δt given the input u_{n+k} . Lastly, we introduced an encoder function ψ_{θ} with encoder lengths n_a and n_b , for the past output and input samples respectively, which estimates the initial states of the considered subsection. A graphical summary of the proposed method called the CT subspace encoder (abbreviated as SUBNET) can be viewed in Figure 1.

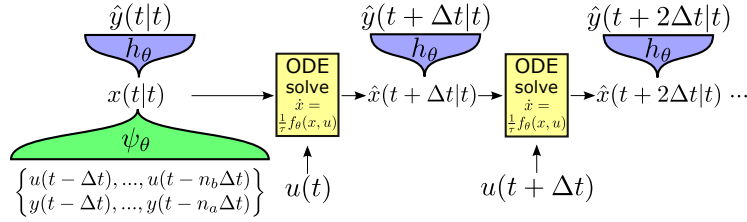


Fig. 1: The CT subspace encoder (SUBNET) method applied on a subsection of the data of length $T\Delta t$ where the encoder ψ_{θ} estimates the initial state, h_{θ} provides the output predictions while $\frac{1}{\tau} f_{\theta}$ governs the state dynamics.

The first observation is that optimization problem (3) is a generalisation of (2) since if $T = N$ and $n_a = n_b = 0$, the original optimization problem (2) is recovered. However, as one might observe, this optimization problem is less computationally challenging to solve if $T < N$ since the first sum can be computed in parallel. Moreover, since the subsections are relatively short, any instabilities have less time to develop increasing the stability of the value and the gradient of $x(t)$ [25]. Lastly, one can construct batches by using only a subset of available subsections enabling batch optimization.

An error in the initial state of $x_{n|n}$ can significantly bias the estimate due to the short nature of the subsections. To counter this, we formulated an encoder function ψ_{θ} which estimates the initial state of each subsection. This encoder

function does not require any additional loss functions to operate as intended since any reduction in the initial state error automatically also reduces the truncated simulation loss.

It is widely known that input and output normalization is essential for obtaining good models throughout deep learning. However, this optimization problem has unknown intermediate variables $x(t)$ and $\dot{x}(t)$. Hence, the function f_θ cannot be normalized conventionally as its (output) distribution is unknown a priori. Hence, through a similar argument as batch-normalization, we introduce a scalar normalization factor $1/\tau$ in front of f_θ . The benchmark experiments show that this normalization factor increases optimization stability and enhances performance when the size of the distributions (i.e. standard deviation) of $x(t)$ and the outputs of f_θ become approximately 1 for some value of $1/\tau$.

4.1 Existence of the encoder and the reconstructability map

The existence of the encoder function is motivated by the recognition that it is an approximation of the reconstructability map. The reconstructability map is the map from past outputs and inputs to the current state which exists under some necessary conditions [19]. In this subsection, we explicitly show that the encoder function is an approximation of the reconstructability map and derive these conditions.

For simplicity of explanation let us first assume that we are estimating an Linear Time-Invariant (LTI) system given by:

$$\begin{aligned}\dot{x}(t) &= A_c x(t) + B_c u(t), \\ y(t) &= C_c x(t) + w(t),\end{aligned}\tag{4}$$

which can be solved as (see: [8]):

$$x(t) = e^{A_c t} x(0) + \int_0^t e^{A_c(t-t')} B_c u(t') dt'. \tag{5}$$

Furthermore, the form of this solution also enables a transformation to an equivalent discrete-time formulation of this LTI system as (assuming ZOH inputs):

$$x_{n+1} = \underbrace{e^{A_c \Delta t}}_A x_n + \underbrace{\int_t^{t+\Delta t} e^{A_c(t-t')} B_c dt'}_B u_n = A x_n + B u_n. \tag{6}$$

This equation can be integrated backwards in time (i.e. inverted) since $\det(A) = e^{\text{tr}(A_c)\Delta t} \neq 0$, which yields the following equations:

$$\begin{aligned}y_{n-1} &= C A^{-1} x_n - C A^{-1} B u_{n-1} + w_{n-1}, \\ y_{n-2} &= C A^{-2} x_n - C A^{-2} B u_{n-1} - C A^{-1} B u_{n-2} + w_{n-2}, \\ &\vdots \\ y_{n-z} &= C A^{-z} x_n - C A^{-z} B u_{n-1} \dots - C A^{-1} B u_{n-z} + w_{n-z}, \\ Y_n^{-z} &= C A x_n - C A B U_n^{-z} + W_n^{-z},\end{aligned}\tag{7}$$

where $Y_n^{-z} = [y_{n-1}^\top \ y_{n-2}^\top \ \dots \ y_{n-z}^\top]^\top$, $U_n^{-z} = [u_{n-1}^\top \ u_{n-2}^\top \ \dots \ u_{n-z}^\top]^\top$, $W_n^{-z} = [w_{n-1}^\top \ w_{n-2}^\top \ \dots \ w_{n-z}^\top]^\top$, C_A the observability matrix and C_{AB} defined as:

$$C_A = \begin{pmatrix} CA^{-1} \\ CA^{-2} \\ \vdots \\ CA^{-z} \end{pmatrix}, \quad C_{AB} = \begin{pmatrix} CA^{-1}B & 0 & \dots & 0 \\ CA^{-2}B & CA^{-1}B & \dots & 0 \\ \vdots & \vdots & \ddots & \vdots \\ CA^{-z}B & CA^{-z+1}B & \dots & CA^{-1}B \end{pmatrix}. \quad (8)$$

As one can observe, equation 7 has an exact solution for x_n if C_A is invertible and if W_n^{-z} is known. However, in practise W_n^{-z} is unknown and this equation cannot be solved directly. For the case that W_n^{-z} is unknown one can approximate the state $\hat{x}_n \approx x_n$ solving the following linear regression problem

$$\hat{x}_n = \arg \min_{\hat{x}_n} \|Y_n^{-z} - C_A \hat{x}_n + C_{AB} U_n^{-z}\|_2.$$

This optimization problem has a unique solution if and only if $C_A^T C_A$ is full rank, which also provides the necessary condition that $zn_y \geq n_x$. Moreover, the estimate \hat{x}_n is an unbiased estimate of x_n and it converges to the real value of $\hat{x}_n \rightarrow x_n$ for $z \rightarrow \infty$ under mild conditions [19]. This shows that there exists an optimal linear mapping $\hat{x}_n = \psi(U_n^{-z}, Y_n^{-z})$ for the LTI case which is known as the reconstructability map.

A similar conclusion can be obtained by considering the nonlinear case for which one can transform the equation to discrete-time in a similar way

$$\dot{x}(t) = f(x(t), u(t)) \rightarrow x_{n+1} = f_d(x_n, u_n) \rightarrow x_{n-1} = f_d^{-1}(x_n, u_{n-1}) \quad (9)$$

where here f_d^{-1} always exists by recognising that the Picard–Lindelöf theorem holds since f is uniformly Lipschitz continuous in x for all u [22] which is one of our starting assumptions. Just as before, the past outputs can be computed given the current state as:

$$\begin{aligned} y_{n-1} &= (h \circ f_d^{-1})(x_n, u_{n-1}) + w_{n-1} \\ y_{n-2} &= (h \circ f_d^{-2})(x_n, u_{n-1}, u_{n-2}) + w_{n-2} \\ &\vdots \\ y_{n-z} &= (h \circ f_d^{-z})(x_n, u_{n-1}, u_{n-2}, \dots, u_{n-z}) + w_{n-z} \\ Y_n^{-Z} &= (H \circ F_d^{-z})(x_n, U_n^{-z}) + W_n^{-z} \end{aligned} \quad (10)$$

where

$$f_d^{-p}(x_n, u_{n-1}, \dots, u_{n-p}) = f_d^{-p+1}(f_d^{-1}(x_n, u_{n-1}), u_{n-2}, \dots, u_{n-p})$$

is the application of f_d^{-1} , p times to obtain x_{n-p} .

Eq. (10) can be solved for x_n since this equation is a nonlinear fixed point problem if W_n^{-z} is known. For the case that W_n^{-z} is unknown one can estimate

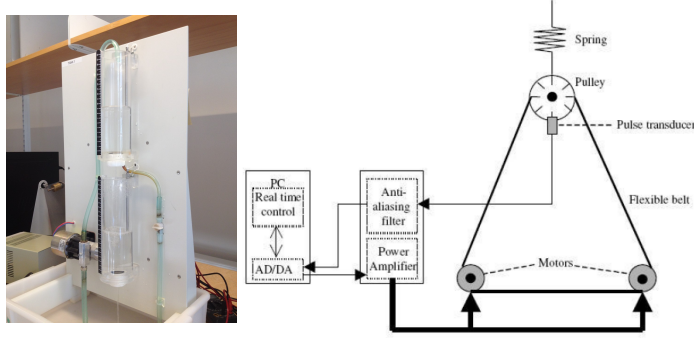


Fig. 2: A photo of the **Cascade Tank with overflow (CCT)** system [30] and a graphical depiction of the **Coupled Electric Drive (CED)** system [32]. These two systems are the basis of the benchmarks used in the analysis and comparison of the proposed method.

the state $\hat{x}_n \approx x_n$ by solving the nonlinear regression problem;

$$\hat{x}_n = \arg \min_{\hat{x}_n} \|Y_n^{-z} - (H \circ F_d^{-z})(\hat{x}_n, U_n^{-z})\|_2, \quad (11)$$

$$= \arg \min_{\hat{x}_n} \|L(\hat{x}_n, Y_n^{-z}, U_n^{-z})\|_2. \quad (12)$$

Hence, a unique reconstructability map exists if f is uniformly Lipschitz continuous and that $(\nabla_x L)^T \nabla_x L$ is full rank in \hat{x}_n .

However, computing the reconstructability map for our model requires solving an optimization problem that becomes computationally infeasible to compute during training. Hence, the encoder function aims to approximate the solution to the optimization problem of the reconstructability map, i.e.

$$\psi_\theta(U_n^{-z}, Y_n^{-z}) \approx \arg \min_{\hat{x}_n} \|Y_n^{-z} - (H \circ F_d^{-z})(\hat{x}_n, U_n^{-z})\|_2.$$

5 Experiments

5.1 Benchmark descriptions

The **Cascade Tank with overflow (CCT)** benchmark [30] consists of measurements taken from a two-tank fluid system with a pump. The input signal controls a water pump that delivers water from the reservoir to the upper tank. Through a small opening in the upper tank, the water enters the lower tank where the water level is recorded. Lastly, through a small opening in the lower tank, the water re-enters the reservoir. This benchmark is nonlinear as the flow rates are governed by square root relations and the flow can overflow either tank which is a hard nonlinearity. The benchmark consists of two datasets with measurements of 1024 samples each. The first dataset will be used for training

and the first 512 samples of the second set for validation (used only for early stopping) and the entire second set for testing. Most of the other methods to which we will compare use the entire second set as validation and test set, as no explicit test set is provided in this benchmark description, hence, even with the overlap this is still a fair comparison.

The **Coupled Electric Drive (CED)** benchmark [32] consists of measurements from a belt and pulley with two motors where both clockwise and counter-clockwise movement is permitted. The motors are actuated by the given inputs and the measured output is a pulse transducer that only measures the absolute velocity (i.e. insensitive to the sign of the velocity) of the belt. The system has approximately three states; the velocity of the belt, the position of the pulley, and the velocity of the pulley. The benchmark consists of two datasets of 500 samples each. The first 300 samples are used for training and the other 200 samples are for testing and of those the first 100 samples are also used for validation with both datasets. Similar to the last benchmark, even with this overlap, it is still a fair comparison for most of the other methods to which we will compare use the entire second set as validation.

5.2 Results

Using the subspace encoder method (3) we estimate a model where the three functions h_θ , f_θ and ψ_θ are implemented as 2 hidden layer neural networks with 64 hidden nodes per layer, tanh activation and a linear bypass from the input to the output similar to a residual connection for both benchmarks. As ODEsolver we use a single RK4 step between samples and assume that the input signal is zero-order hold. As for the implementation of the CT subspace encoder method the following hyper-parameters are considered; $n_x = 2$, $n_a = n_b = 5$ and $T = 30$ for CCT and $n_x = 3$, $n_a = n_b = 4$ and $T = 60$ for CED. These hyperparameters are chosen based on few-step prediction-error figures as was shown in [4]. The training is done by using the Adam optimizer with default settings [20] with a batch size of 32 for CED and 64 for CCT and using a simulation on the validation dataset for early stopping to reduce overfitting. To increase confidence in our results we estimate at least 17 models when doing experiment per hyperparameter setting for both benchmarks.

We also directly compare to a reproduction of neural ODE on both benchmarks. We adapt the code and the example (“`latent.ODE.py`”) available online [9] to include ZOH inputs, leaving the neural network unaltered and an RK4 integrator. We observed that the initial model was unstable (resulting in NaN values) and, hence, the neural ODE method alone was unable to result in any reasonable model. To stabilize the neural ODE method we also introduce a state-derivative normalization term $1/\tau$ similar as in the proposed method (3). The value of $1/\tau$ for CCT and CED for neural ODE was initially chosen to be the optimal value found in the CT encoder approach, however, in the CED case, it was lowered to increase stability. These values can be viewed in the upcoming

table. Lastly, we obtained an ensemble of 24 models for CCT and 8 models for CED.³

We compared our obtained model to the literature in Table 1. The table shows that the obtained models with the CT subspace encoder method are state-of-the-art. These results are obtained using unrestrained state-space and fully connected neural networks as model elements. Remarkably, the resulting performance is quite close to the performance of the grey-box model. Furthermore, Figure 3 illustrates that the resulting models have been able to model the non-linear behavior present in both benchmarks. We do not observe overfitting in the first section which was used for validation.

Table 1: The test simulation error on two benchmarks for the CT subspace encoder method using an ensemble of models. The value given is the best RMS of all estimated models and the value between parentheses is the mean performance of the model. Note that we are unable to report the results for the neural ODE without state-derivative normalization since the optimization was unstable.

(a) CCT benchmark		(b) CED benchmark		
Method	RMS	Method	RMS [ticks/s]	
			Set 1	Set 2
BLA [24]	0.75	RBFNN - FSDE [1]	0.130	0.185
Volterra model [5]	0.54	GP with rational quadratic kernel [35]	0.150	0.167
State-space with GP-inspired prior [31]	0.45	GP with squared exponential kernel [35]	0.153	0.132
SCI [13]	0.40	Sparse Bayesian MLP [35]	0.149	0.120
NL-SS + NLSS2 [24]	0.34		(0.187)	(0.134)
TSEM [13]	0.33	Cascaded Splines [29]	0.216	0.110
Tensor B-splines [17]	0.30	Sparse Bayesian LSTM [35]	0.121	0.097
neural ODE [9] with normalization ($\Delta t/\tau = 0.03$)	0.18		(0.155)	(0.126)
Grey-Box with physical overflow model [26]	0.18	Extended Fuzzy Logic [28]	0.150	0.092
CT subspace encoder	0.22	neural ODE [9] with normalization ($\Delta t/\tau = 0.12$)	0.131	0.086
($\Delta t/\tau = 0.032$)	(0.30)		(0.198)	(0.158)
		CT subspace encoder	0.115	0.074
		($\Delta t/\tau = 0.3$)	(0.143)	(0.100)

Table 1 also contains neural ODE with normalization. Only a small fraction of the estimated neural ODE with normalization models was able to get comparable results to the state-of-the-art. This is a small fraction since the optimization often resulted in models which did not generalize well to the test set. We think that this is due to the availability of only a single sequence in the training set for the CCT benchmark (and two sequences for CED) which results in extensive overfitting.

³ The code used for both subspace encoder and neural ODE experiments is available at <https://github.com/GerbenBeintema/encoder-CT-ode-ecml-2022>

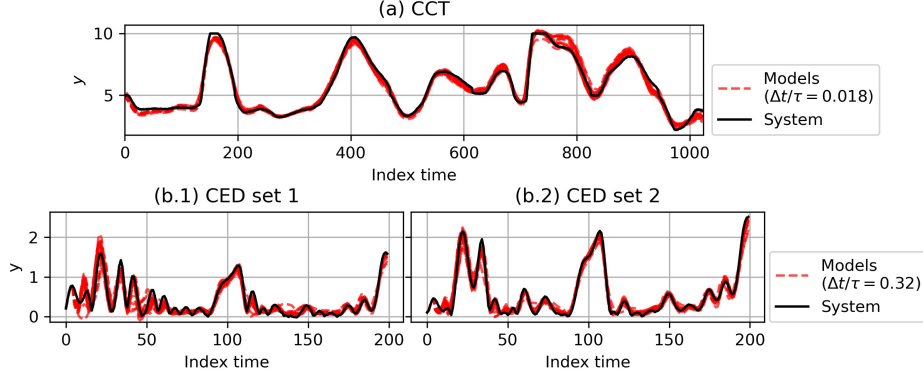


Fig. 3: The time-domain simulation using the obtained models for the CT encoder method with a given $\Delta t/\tau$ (3) can make accurate long term predictions. The CED benchmark is split since it contains two test sequences.

In comparison, the subspace encoder method is less prone to overfitting since it uses many subsections of the available sequence(s). Moreover, the subspace encoder method only requires about 20 minutes to train a model to the lowest validation loss, whereas, neural ODE requires about 2 hours for CED and 5 hours for CCT.

When we introduced the state-derivative normalization factor $1/\tau$, we stated that if it normalized f_θ it increased optimization stability and the quality of the obtained models. We provide experimental insight for these two statements by providing a parameter sweep over $\Delta t/\tau$. Moreover, to eliminate variations due to different initial parameters we trained an ensemble of models which creates box-plots with $|f| = 1/N \sum_n \|f_\theta(x_n, u_n)\|_2$, $|x| = 1/N \sum_n \|x_n\|_2$ and the RMS simulation error. These box-plots as shown in Figure 4 indeed illustrates that if $|f| \approx |x| \approx 1$ for some normalization factor $\Delta t/\tau$, the lowest RMS simulation error is obtained validating our argument.

6 Conclusion

In this paper we considered the problem of CT model identification including latent states, external inputs and measurement noise for which we formulated the subspace encoder method. We showed that the proposed method is able to obtain state-of-the-art CT models consisting of only fully connected neural networks. This method has been derived after analysis of the classical CT optimization problem which recognised and, hence, solved multiple issues. These issues were, computational cost and stability of the optimization problem, bias induced by initial state errors and un-normalized state derivatives. Hence, we resolved these issues by altering the optimization problem to consider multiple subsections where the initial state is estimated with an encoder function and a state derivative normalization term. This work only considers the state

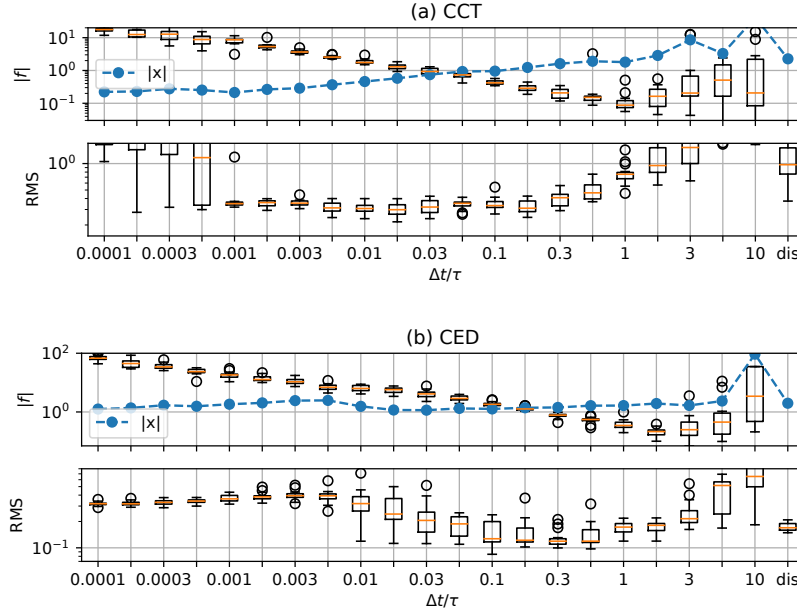


Fig. 4: On the CCT and CED benchmarks there exists a range of state-derivative normalization factors ($\dot{x} = \frac{1}{\tau}f_{\theta}(x, u)$) where $|f| \approx |x| \approx 1$ the CT encoder method (3) has significantly improved the RMS simulation error.

derivative normalization term as a hyperparameter but future research might be able to formulate a online method of estimating the term similar to batch-normalization. Lastly, through careful analysis using properties of ODEs, we show that the existence of the encoder function has the necessary condition that the state-derivatives are Lipschitz continuous.

References

1. Ayala, H.V.H., da Cruz, L.F., Freire, R.Z., dos Santos Coelho, L.: Cascaded free search differential evolution applied to nonlinear system identification based on correlation functions and neural networks. In: 2014 IEEE Symposium on Computational Intelligence in Control and Automation (CICA). pp. 1–7. IEEE (2014)
2. Ayed, I., de Bézenac, E., Pajot, A., Brajard, J., Gallinari, P.: Learning dynamical systems from partial observations. Second Workshop on Machine Learning and the Physical Sciences, NeurIPS (2019), <http://arxiv.org/abs/1902.11136>
3. Bai, S., Kolter, J.Z., Koltun, V.: Deep equilibrium models. Advances in Neural Information Processing Systems **32** (2019)
4. Beintema, G., Toth, R., Schoukens, M.: Nonlinear state-space identification using deep encoder networks. In: Learning for Dynamics and Control. pp. 241–250. PMLR (2021)

5. Birpoutsoukis, G., Csurscia, P.Z., Schoukens, J.: Efficient multidimensional regularization for volterra series estimation. *Mechanical Systems and Signal Processing* **104**, 896–914 (2018)
6. Brajard, J., Carrassi, A., Bocquet, M., Bertino, L.: Combining data assimilation and machine learning to emulate a dynamical model from sparse and noisy observations: A case study with the lorenz 96 model. *Journal of Computational Science* **44**, 101171 (2020)
7. Brunton, S.L., Proctor, J.L., Kutz, J.N.: Discovering governing equations from data by sparse identification of nonlinear dynamical systems. *Proceedings of the national academy of sciences* **113**(15), 3932–3937 (2016)
8. Callier, F.M., Desoer, C.A.: *Linear system theory*. Springer Science & Business Media (2012)
9. Chen, R.T., Rubanova, Y., Bettencourt, J., Duvenaud, D.K.: Neural ordinary differential equations. *Advances in neural information processing systems* **31** (2018)
10. Cranmer, M., Greydanus, S., Hoyer, S., Battaglia, P., Spergel, D., Ho, S.: Lagrangian neural networks. *ICLR 2020* (2020)
11. De Brouwer, E., Simm, J., Arany, A., Moreau, Y.: Gru-ode-bayes: Continuous modeling of sporadically-observed time series. *Advances in neural information processing systems* **32** (2019)
12. Fan, F.L., Xiong, J., Li, M., Wang, G.: On interpretability of artificial neural networks: A survey. *IEEE Transactions on Radiation and Plasma Medical Sciences* **5**(6), 741–760 (2021)
13. Forgione, M., Piga, D.: Continuous-time system identification with neural networks: model structures and fitting criteria. *European Journal of Control* **59**, 69–81 (2021)
14. Garcia, C.E., Prett, D.M., Morari, M.: Model predictive control: Theory and practice—a survey. *Automatica* **25**(3), 335–348 (1989)
15. Grathwohl, W., Chen, R.T., Bettencourt, J., Sutskever, I., Duvenaud, D.: Ffjord: Free-form continuous dynamics for scalable reversible generative models. *ICLR*, arXiv:1810.01367 (2019)
16. Greydanus, S., Dzamba, M., Yosinski, J.: Hamiltonian neural networks. *Advances in Neural Information Processing Systems* **32** (2019)
17. Karagoz, R., Batselier, K.: Nonlinear system identification with regularized tensor network b-splines. *Automatica* **122**, 109300 (2020)
18. Karniadakis, G.E., Kevrekidis, I.G., Lu, L., Perdikaris, P., Wang, S., Yang, L.: Physics-informed machine learning. *Nature Reviews Physics* **3**(6), 422–440 (2021)
19. Katayama, T.: *Subspace methods for system identification*, vol. 1. Springer (2005)
20. Kingma, D.P., Ba, J.: Adam: A method for stochastic optimization. *arXiv preprint arXiv:1412.6980* (2014)
21. Maulik, R., Mohan, A., Lusch, B., Madireddy, S., Balaprakash, P., Livescu, D.: Time-series learning of latent-space dynamics for reduced-order model closure. *Physica D: Nonlinear Phenomena* **405**, 132368 (2020)
22. Murray, F.J., Miller, K.S.: *Existence theorems for ordinary differential equations*. Courier Corporation (2013)
23. Papamakarios, G., Nalisnick, E., Rezende, D.J., Mohamed, S., Lakshminarayanan, B.: Normalizing flows for probabilistic modeling and inference. *Journal of Machine Learning Research* **22**(57), 1–64 (2021)
24. Relan, R., Tiels, K., Marconato, A., Schoukens, J.: An unstructured flexible nonlinear model for the cascaded water-tanks benchmark. *IFAC-PapersOnLine* **50**(1), 452–457 (2017)

25. Ribeiro, A.H., Tiels, K., Umenberger, J., Schön, T.B., Aguirre, L.A.: On the smoothness of nonlinear system identification. *Automatica* **121**, 109158 (2020)
26. Rogers, T., Holmes, G., Cross, E., Worden, K.: On a grey box modelling framework for nonlinear system identification. In: *Special Topics in Structural Dynamics*, Volume 6, pp. 167–178. Springer (2017)
27. Rudy, S.H., Kutz, J.N., Brunton, S.L.: Deep learning of dynamics and signal-noise decomposition with time-stepping constraints. *Journal of Computational Physics* **396**, 483–506 (2019)
28. Sabahi, F., Akbarzadeh-T, M.R.: Extended fuzzy logic: Sets and systems. *IEEE Transactions on Fuzzy Systems* **24**(3), 530–543 (2015)
29. Scarpiniti, M., Comminiello, D., Parisi, R., Uncini, A.: Novel cascade spline architectures for the identification of nonlinear systems. *IEEE Transactions on Circuits and Systems I: Regular Papers* **62**(7), 1825–1835 (2015)
30. Schoukens, M., Mattson, P., Wigren, T., Noel, J.P.: Cascaded tanks benchmark combining soft and hard nonlinearities. In: *Workshop on nonlinear system identification benchmarks*. pp. 20–23 (2016)
31. Svensson, A., Schön, T.B.: A flexible state-space model for learning nonlinear dynamical systems. *Automatica* **80**, 189–199 (2017)
32. Wigren, T., Schoukens, M.: Coupled electric drives data set and reference models. Department of Information Technology, Uppsala Universitet (2017)
33. Zhong, Y.D., Dey, B., Chakraborty, A.: Symplectic ode-net: Learning hamiltonian dynamics with control. *ICLR*, arXiv:1909.12077 (2020)
34. Zhou, H., Zhang, S., Peng, J., Zhang, S., Li, J., Xiong, H., Zhang, W.: Informer: Beyond efficient transformer for long sequence time-series forecasting. In: *Proceedings of AAAI* (2021)
35. Zhou, H., Ibrahim, C., Zheng, W.X., Pan, W.: Sparse bayesian deep learning for dynamic system identification. *arXiv preprint arXiv:2107.12910* (2021)